

A controllable approach for the synthesis of titanate derivatives of potassium tetratitanate fiber

MING HE, XIN FENG, XIAOHUA LU*, XIAOYAN JI, CHANG LIU, NINGZHONG BAO, JINGWEI XIE

Department of Chemical Engineering, Nanjing University of Technology, Nanjing, Jiangsu 210009, People's Republic of China
E-mail: xhlu@njuct.edu.cn

Three types titanate derivatives, $K_2Ti_6O_{13}$ fiber, $K_2Ti_8O_{17}$ fiber and anatase TiO_2 fiber, were synthesized by ion-exchange reaction from potassium tetratitanate fiber ($K_2Ti_4O_9$) based on the hydrate conditions predicted by a thermodynamic model. These products were formed by a heat treatment of the corresponding hydrate intermediates $K_{1.33}H_{0.67}Ti_4O_9 \cdot H_2O$, $KHTi_4O_9 \cdot 0.5H_2O$ and $H_2Ti_4O_9 \cdot 1.2H_2O$ which were quantitatively obtained by controlling the pH value and the equilibrium concentration of potassium ion. The mole ratio of Ti/K in solid phase (R) of the target products was taken as the controlling aim in the hydrate process. The temperature for heat treatment of hydrate intermediates was determined by thermogravimetry (TG) and differential scanning calorimetry (DSC). All products retained fibrous morphology similar to that of $K_2Ti_4O_9$ used as the starting material.

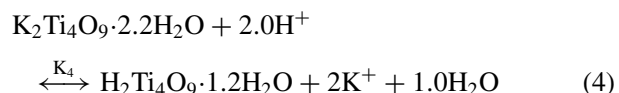
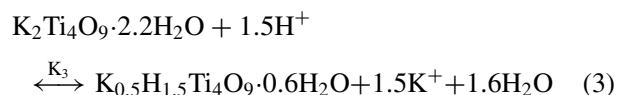
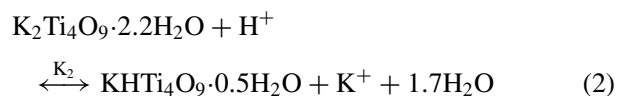
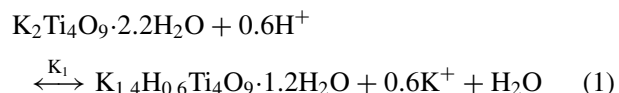
© 2004 Kluwer Academic Publishers

1. Introduction

Titanates, typically potassium titanate fibers ($K_2O \cdot nTiO_2$ with $n = 2, 4, 6$ and 8), have been regarded as novel functional materials. Titanates with $n = 2$ and 4 , potassium dititanate ($K_2Ti_2O_5$) and potassium tetratitanate ($K_2Ti_4O_9$) fibers possess layered structure and have great ion-exchange abilities, are used as inorganic ion exchangers and precursors converted to other alkali-metal titanates [1]. Titanates with $n = 6$ and 8 , potassium hexatitanate ($K_2Ti_6O_{13}$) and potassium octatitanate ($K_2Ti_8O_{17}$) fibers are advanced reinforcing materials for the composite and frictional materials for brakes [2]. Layered protonic tetratitanate ($H_2Ti_4O_9 \cdot 1.2H_2O$), the proton form of $K_2Ti_4O_9$, is known to be applicable as inorganic ion exchanger [3], photochemical catalyst [4, 5] and layered host framework to synthesize inorganic-organic nanocomposite materials [6, 7]. Especially anatase TiO_2 fiber is often used as support and photocatalyst [8]. These titanate derivatives can be synthesized by ion-exchange reaction method, which consists of the hydrolysis of $K_2Ti_2O_5$ or $K_2Ti_4O_9$ followed by filtration and thermolysis [1, 9]. However, it is difficult to produce pure titanate derivatives because the content of potassium ions of the hydrate intermediates can not be accurately controlled in the process of hydrolysis.

For the hydration process from $K_2Ti_4O_9$, potassium ions are stepwise replaced with protons in the acid solution while several hydrate intermediates appear.

The ion-exchange reaction can be written as following Equations 1 to 4:



where $K_2Ti_4O_9 \cdot 2.2H_2O$ is the solid phase when $K_2Ti_4O_9$ fiber exists in aqueous solutions and the hydrate intermediate is expressed as $K_{2-b}H_bTi_4O_9 \cdot nH_2O$ ($0 < b \leq 2$).

For these ion-exchange reactions, many factors, such as the pH value, the amount of water, the concentration of the ions in aqueous phase and the reaction time, affect the composition of the hydrate intermediates. Recently Bao *et al.* [10] proposed a thermodynamic model for the ion-exchange reaction process from $K_2Ti_4O_9$ fiber and suggested that all above mentioned factors could be come down to the combination affection of the pH value

*Author to whom all correspondence should be addressed.

and the equilibrium concentration of K^+ ion (m_K). In their paper, the value of equilibrium constant for each reaction and mole fraction of each solid phase (x_i) was calculated and the proposed model was used to predict hydrate conditions for the synthesis of $K_2Ti_6O_{13}$ and TiO_2 . However, the predicted hydrate conditions were not very specific and only several scatter predicted conditions were reached.

Based on this, in the present study, the mole ratio of Ti/K in solid phase (R) of the target products was taken as the controlling aim and the hydrate corresponding intermediates were obtained by controlling the pH value and m_K in the hydrate process. For example, R of $K_2Ti_8O_{17}$ is 4, that is to say, the mole ratio of Ti/K of the corresponding intermediate must be controlled as 4 by controlling the pH value and m_K . The hydrate conditions were very clear and could be directly reached. To investigate the phase transformation of the hydrate intermediates, thermogravimetry (TG) and differential scanning calorimetry (DSC) were performed. Thus the single-phase derivatives of $K_2Ti_4O_9$, $K_2Ti_6O_{13}$ fiber, $K_2Ti_8O_{17}$ fiber and anatase TiO_2 fiber could be controllably synthesized by ion-exchange method.

2. Prediction of the hydrate conditions

When corresponding equilibrium constants are determined and equilibrium composition in liquid phase is monitored, mole fraction of each solid phase (x_i) can be calculated. Then the equilibrium composition of all hydration intermediates is converted to the mole ratio of Ti/K in solid phase (R). The expression is shown as following:

$$R = \frac{4}{2 \left(1.0 - \sum_{i=1}^N x_i \right) + \left(\sum_{i=1}^N \cdot (2 - b) \cdot x_i \right)} \quad (5)$$

where N is the number of solid phases except $K_2Ti_4O_9 \cdot 2.2H_2O$ at equilibrium, b is stoichiometric coefficient, x_i is the mole fraction of each solid phase. So R can be regarded as a function of the pH value and the concentration of K^+ ion, which can be drawn as a contour map (Fig. 1).

In Fig. 1, the horizontal axis of the contour map corresponds to the pH value of equilibrium, the vertical axis corresponds to the equilibrium concentration of K^+ ion (m_K) and the levels labeled on the curved lines of the contour map correspond to the mole ratio of Ti/K in solid phase (R). The range of the pH value in the model is chosen at $2 < \text{pH} < 14$ for titanium can be extracted at acid concentration $> 0.05 \text{ M}$ [9].

From Fig. 1, it is obvious that pH value and m_K have a great influence on R . As expected, the curves labeled 3 and 4 correspond to the yield regions of hydrate intermediates with the mole ratio of Ti/K are at 3 and 4. It is also means that the corresponding pH value and m_K are the synthetic conditions for $K_2Ti_6O_{13}$ and $K_2Ti_8O_{17}$. Moreover, the pH value has greater influence on R than m_K does because the curve is almost vertical when in the region of higher concentration of K^+ ion. So when the fibers are synthesized by ion-exchange method under industrial synthesis condition, higher concentration

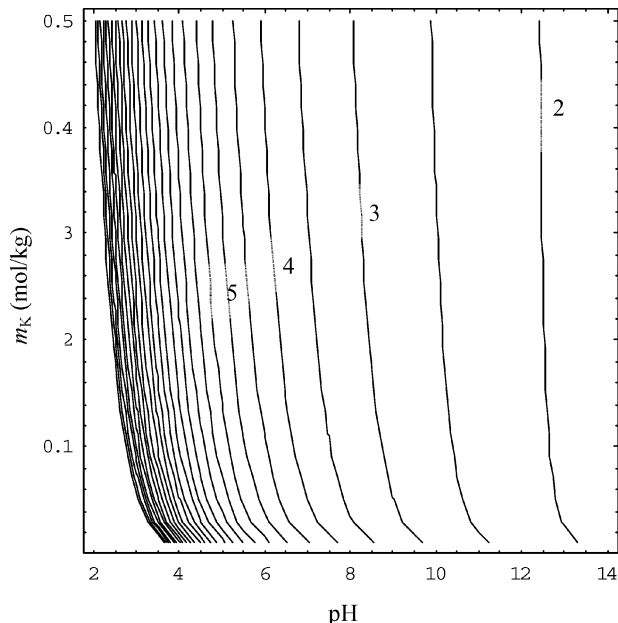


Figure 1 Contour map of the predicted hydration conditions showing the Ti/K molar ratio in the solid phase (R) is relative to the pH value and the equilibrium concentration of K^+ ion.

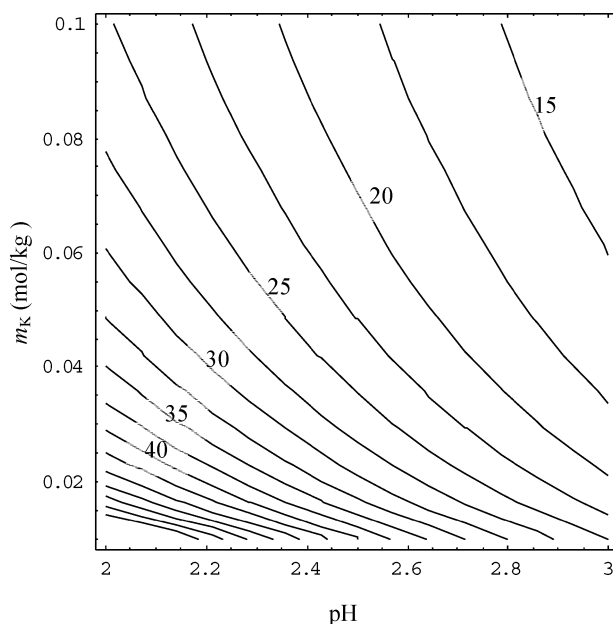


Figure 2 The partial contour map of the predicted hydration conditions of higher Ti/K molar ratio in the solid phase (R) when at low pH value and low equilibrium concentration of K^+ ion.

of K^+ ion may be chosen if m_K can't be accurately monitored.

In the case of the ion-exchange solid products with a higher R is generated at lower values of pH and m_K . It is apparently shown in the partial contour map (Fig. 2). The contour lines in Fig. 2 are denseness because the pH value and m_K have a great influence on R . For the synthesis of pure TiO_2 , R must be controlled higher than 20 ($K \ll Ti$). In this process, lower m_K can be obtained by treating with fresh HCl for several times at low pH value. For example, $R > 20$ can be obtained at $m_K < 0.02$ with $\text{pH} < 3$ or at $m_K < 0.1$ with $\text{pH} < 2.3$. It is also can be observed from Fig. 2 that m_K has a wide controlling range when the pH value is close to

2, so it prefer choosing low pH value when synthesize TiO_2 .

Based on the hydrate conditions from Figs 1 and 2, pure TiO_2 fiber, $\text{K}_2\text{Ti}_6\text{O}_{13}$ fiber and $\text{K}_2\text{Ti}_8\text{O}_{17}$ fiber can be obtained at $\text{pH} = 2.0$ with $m_{\text{K}} < 0.1$ M, $\text{pH} = 9$ with $m_{\text{K}} = 0.06$ M and $\text{pH} = 6.5$ with $m_{\text{K}} = 0.14$ M respectively.

3. Experimental procedure

3.1. Production of initial material

K_2CO_3 (Reagent grade) were mixed with the concentrated hydrous titania ($\text{TiO}_2 \cdot n\text{H}_2\text{O}$) at the $\text{TiO}_2/\text{K}_2\text{O}$ molar ratio of 3.0. The mixture was dried in an oven at 90°C for 10 h. Potassium tetratitanate fiber ($\text{K}_2\text{Ti}_4\text{O}_9$), was prepared by sintering the dried mixture in a muffle furnace at 960°C for 10 h [11]. All samples were taken out at the end of holding time and cooled in air.

3.2. Production of the derivatives of $\text{K}_2\text{Ti}_4\text{O}_9$ fiber

Fibrous $\text{K}_2\text{Ti}_4\text{O}_9$ was suspended in vigorously stirred water simultaneously with adding 1 M HCl continuously. The corresponding hydrate conditions were determined according to the prediction results. The pH value was detected on-line by the pH meter and the relevant equilibrium concentration of K^+ ion was determined by ion selective electrode [12] and controlled by adding 1 M KCl. After the equilibrium was attained, the hydration intermediates were separated by filtration and washed with distilled water, followed by drying at room temperature in a desiccator. With further treated of intermediates at various temperatures in muffle furnace for 2 h, the derivatives of $\text{K}_2\text{Ti}_4\text{O}_9$ were obtained.

3.3. Instruments and characterization of the solid phase

In this work, the K membrane ISE (Model 401, China) and chloride solid-state ISE (Model 301, China) were used in the measurements of activity of K^+ and equilibrium concentration was calculated with the suitable activity coefficient [13]. A SCHOTT-GERÄTE pH-meter (Model CG0841, Germany) was used to monitor the potential of the cell having a resolution 0.1 mV. A SCHOTT-GERÄTE resistant thermometer (Model W5791 NN, Germany) was used to measure the temperature of the solution and its resolution is 0.1 K.

Phase constitutions of the hydration intermediates and the target products were examined by X-ray diffraction analysis (D8 Advance, BRUKER, Germany) with Ni-filtered $\text{Cu K}\alpha$ radiation. The data were collected over the 2θ range of $5\text{--}60^\circ$ at a rate of 3°min^{-1} . The phase transition temperature were determined by Differential scanning calorimetry (DSC) and thermogravimetric analysis (TGA) (NETZSCH STA 449C Germany), which were performed on dried powders in flowing nitrogen ($30 \text{ cm}^3/\text{min}$) over a wide temperature range

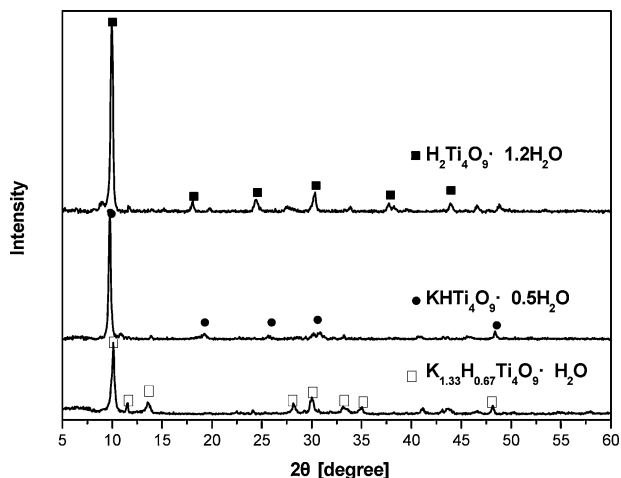


Figure 3 XRD patterns of the hydration intermediates $\text{K}_{1.33}\text{H}_{0.67}\text{Ti}_4\text{O}_9 \cdot \text{H}_2\text{O}$, $\text{KHTi}_4\text{O}_9 \cdot 0.5\text{H}_2\text{O}$ and $\text{H}_2\text{Ti}_4\text{O}_9 \cdot 1.2\text{H}_2\text{O}$.

of $25\text{--}1100^\circ\text{C}$ with a heating rate of $10^\circ\text{C}/\text{min}$. The morphologies and microstructures of the target products were examined by scanning electron microscope (SEM) (JSM-6300, Jeol, Japan).

4. Synthesis results and discussion

4.1. Characterization of the intermediate products

Fig. 3 shows the X-ray powder diffraction patterns of the hydrate intermediate products. According to the prediction results, when R was controlled as 3, 4 and >20 , the intermediates were identified as $\text{K}_{1.33}\text{H}_{0.67}\text{Ti}_4\text{O}_9 \cdot \text{H}_2\text{O}$, $\text{KHTi}_4\text{O}_9 \cdot 0.5\text{H}_2\text{O}$ and $\text{H}_2\text{Ti}_4\text{O}_9 \cdot 1.2\text{H}_2\text{O}$. The intermediate $\text{K}_{1.33}\text{H}_{0.67}\text{Ti}_4\text{O}_9 \cdot \text{H}_2\text{O}$ might be considered as the composite phase of the equilibrium components $\text{KHTi}_4\text{O}_9 \cdot 0.5\text{H}_2\text{O}$ and $\text{K}_{1.4}\text{H}_{0.6}\text{Ti}_4\text{O}_9 \cdot 1.2\text{H}_2\text{O}$. The basic framework of intermediates is built up from a structure unit of four TiO_6 octahedral arranged in lines by means of edge and corner sharing [3]. The interlayered potassium ions are very easily extracted by proton or hydronium ion with acid solution treatment. The reflection peaks appearing around the 2θ value of 10° are from the (200) plane and are attributed to the interlayer distance [3]. It was obvious that the interlayer distance of hydrate intermediates continuously changed when the ion-exchange proceeded, while the host framework was not destroyed. It is suggested that the interlayer distance, which continuously changed during the process, is affected by the content of potassium ions and water molecules in the interlayer.

4.2. Phase transformation of the intermediate products

Fig. 4 shows the TG and DSC profiles of the hydrate intermediates $\text{K}_{1.33}\text{H}_{0.67}\text{Ti}_4\text{O}_9 \cdot \text{H}_2\text{O}$, $\text{KHTi}_4\text{O}_9 \cdot 0.5\text{H}_2\text{O}$ and $\text{H}_2\text{Ti}_4\text{O}_9 \cdot 1.2\text{H}_2\text{O}$, respectively. The samples showed a weight loss accompanied with endo- and exothermic peaks over a wide temperature range of $25\text{--}1100^\circ\text{C}$.

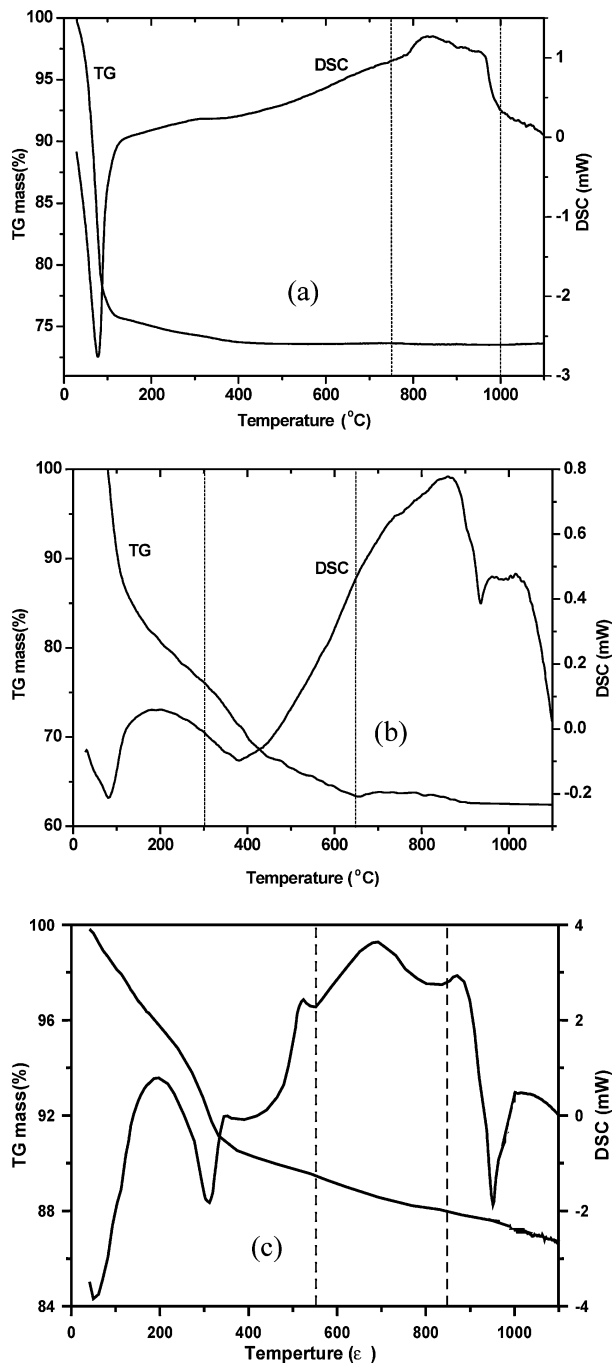


Figure 4 TG and DSC profiles of the hydration intermediates: (a) $K_{1.33}H_{0.67}Ti_4O_9 \cdot H_2O$, (b) $KHTi_4O_9 \cdot 0.5H_2O$ and (c) $H_2Ti_4O_9 \cdot 1.2H_2O$ prepared by the ion-exchange reaction of $K_2Ti_4O_9$.

Fig. 4a shows TG and DSC profile of the hydrate intermediate $K_{1.33}H_{0.67}Ti_4O_9 \cdot H_2O$. The first weight loss of ca. 24% in the range of 40–120°C, where there is an evident endothermic peak, is attributed to the loss of adsorbed water. In the range of 120–420°C, there is a second weight loss of about 3%, which is attributed to the loss of hydration water. The exothermic peak appearing in the range of 750–1000°C in the DSC curve, which is denoted with the dashed lines, is due to the crystallization of $K_2Ti_6O_{13}$.

In Fig. 4b for $KHTi_4O_9 \cdot 0.5H_2O$, noticeable two-stepped losses (step I, 40–120°C, and step II, 300–650°C) and two endothermic peaks are also attributed to the dehydration reactions of adsorbed water and hydration water, accompanied with the crystallization of

$K_2Ti_8O_{17}$. Above 600°C, $K_2Ti_8O_{17}$ tended to decompose to $K_2Ti_6O_{13}$ and anatase TiO_2 [14], accompanied with a strong exothermic peak observed around 800°C in the DSC curve, indicating that $K_2Ti_8O_{17}$ is thermally unstable. When at 950°C, rutile TiO_2 was formed accompanied with an exothermic peak.

Fig. 4c represents the TG-DSC curves of the layered protonic titanate $H_2Ti_4O_9 \cdot 1.2H_2O$. The weight loss is found to extend over a wide temperature range because of the slow dehydration process. The first step up to 200°C is certainly due to the dehydration of water, corresponding to $H_2Ti_8O_{17}$ appears. Above 300°C, a sharp weight loss of about 3% with an endothermic peak is observed, indicating the loss of hydration water and the phase transformation to the monoclinic titania. A strong exothermic peak in the temperature range from 550 to 850°C indicates that the monoclinic titania is transformed to anatase. The last exothermic peak at 1000°C is due to the phase transformation to rutile. This transformation behavior of $H_2Ti_4O_9 \cdot 1.2H_2O$ is similar to that reported by Yin *et al.* [15] although the phase transformation temperatures are a slightly different. All of the results obtained allow us to confirm that the layered hydrate intermediates are easily collapsed to produce derivative phases after dehydration. On heating, the TiO_6 octahedral is rotated by absorption of energy, and then layer structure is transform to tunnel structure [16].

4.3. Characterization of the target products

According to the thermal analysis, $K_2Ti_6O_{13}$ fiber, $K_2Ti_8O_{17}$ fiber and TiO_2 fiber were synthesized by heat treatment of $K_{1.33}H_{0.67}Ti_4O_9 \cdot H_2O$, $KHTi_4O_9 \cdot 0.5H_2O$ and $H_2Ti_4O_9 \cdot 1.2H_2O$ for 2 h at 850°C, 500°C and 800°C, respectively. The XRD pattern of the resultant fibrous products (Fig. 5) definitely exhibited only single-phase products and good crystallinity. The hydration conditions, hydrate intermediates, temperature for heat treatment and the target products are listed in Table I. Fig. 6 shows scanning electron microscopy (SEM) micrographs of hydrate reactants $K_2Ti_4O_9$ (A) and its derivatives $K_2Ti_6O_{13}$ (B), $K_2Ti_8O_{17}$ (C) and

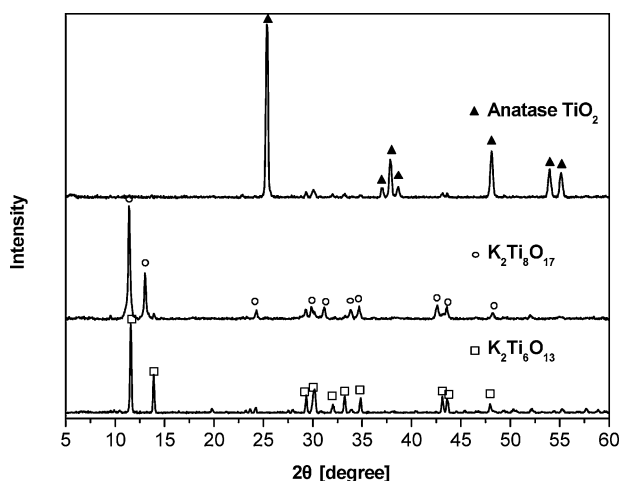


Figure 5 XRD patterns of the target products $K_2Ti_6O_{13}$ fiber, $K_2Ti_8O_{17}$ fiber and anatase TiO_2 fiber.

TABLE I Synthesis of the hydrous intermediates and the target products according to the prediction hydration conditions

R^a	Prediction conditions		Hydrate intermediates	Temperature for heat treatment	Target products
	pH	m_K (mol/kg)			
3	9	0.06	$K_{1.33}H_{0.67}Ti_4O_9 \cdot H_2O$	850°C	$K_2Ti_6O_{13}$
4	6.5	0.14	$KHTi_4O_9 \cdot 0.5H_2O$	500°C	$K_2Ti_8O_{17}$
>20	2	<0.01	$H_2Ti_4O_9 \cdot 1.2H_2O$	800°C	Anatase TiO_2

^aTi/K mole ratio in solid phase.

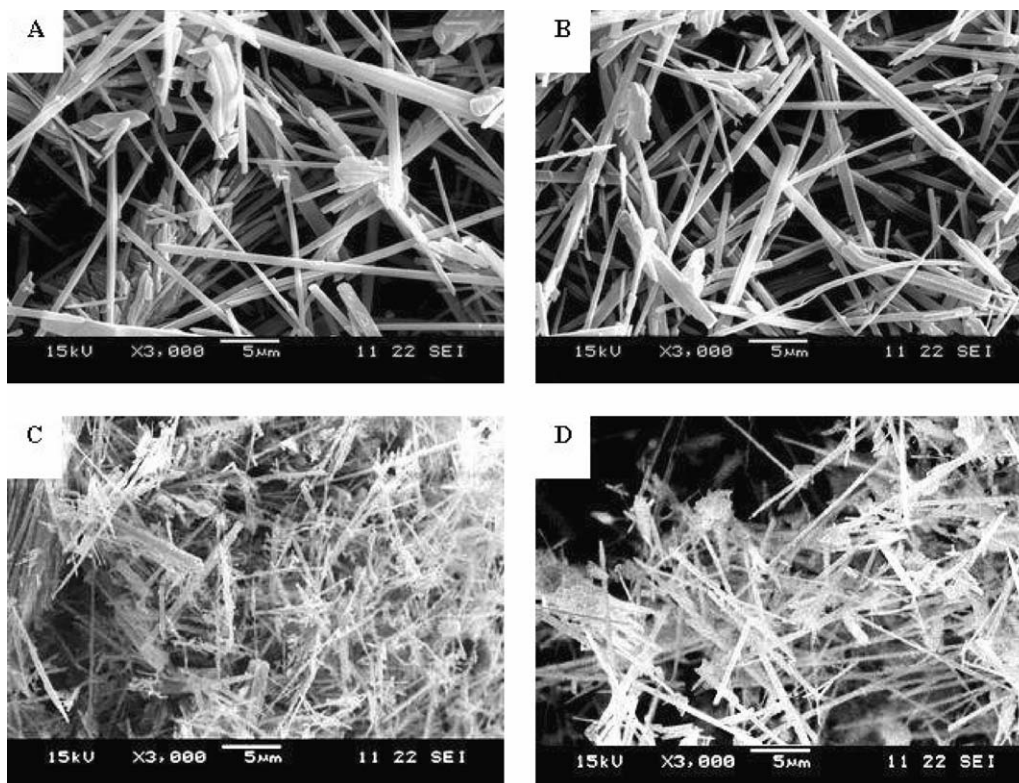


Figure 6 SEM photograph of hydrate reactant: (A) $K_2Ti_4O_9$ and its derivatives, (B) $K_2Ti_6O_{13}$, (C) $K_2Ti_8O_{17}$, and (D) TiO_2 fibers.

TiO_2 (D). The length and diameter of the fibers are 10–30 μm and 0.2–1 μm . All the samples possess fibrous structure indicating that the hydration process does not obviously affect the morphology.

5. Conclusions

The single-phase derivatives of $K_2Ti_4O_9$ fiber, $K_2Ti_6O_{13}$ fiber, $K_2Ti_8O_{17}$ fiber and anatase TiO_2 fiber, were synthesized by ion-exchange method based on the thermodynamic model. When the mole ratio of Ti/K in solid phase were controlled at 3, 4 and >20 in the hydration process by adjusting the pH value and the equilibrium concentration of K^+ ion, the hydrate intermediates $K_{1.33}H_{0.67}Ti_4O_9 \cdot H_2O$, $KHTi_4O_9 \cdot 0.5H_2O$ and $H_2Ti_4O_9 \cdot 1.2H_2O$ were obtained respectively. The phase transformation temperatures for these intermediates were determined at 850°C, 500°C and 800°C by thermal analysis. All the target products possessed a fibrous structure similar to that of $K_2Ti_4O_9$ which used as a starting material.

Acknowledgments

Authors thank the Natural Science Foundation of Jiangsu Province of P. R. China (No. BJ98060), the Outstanding Youth Fund of National Natural Science Foundation of P. R. China (No. 29925616) and the National Natural Science Foundation of P. R. China (No. 20246002 and 20236010).

References

1. Y. FUJIKI and T. OHSAKA, *Yogyo Kyokaishi*. **90** (1982) 19.
2. J. LU and X. LU, *J. Appl. Polym. Sci.* **82** (2001) 368.
3. T. SASAKI, M. WATANABE, Y. KOMATSU and Y. FUJIKI, *Inorg. Chem.* **24** (1985) 2265.
4. M. YANAGISAWA, S. UCHIDA, S. YIN and T. SATO, *Chem. Mater.* **13** (2001) 174.
5. Z. YANG, N. BAO, C. LIU, X. FENG, J. XIE, X. JI and X. LU, *Chem. J. Chinese. U* **23** (2002) 1371.
6. C. AIROLDI, L. M. NUNES and R. F. FARIAS, *Mater. Res. Bull.* **35** (2000) 2081.
7. M. OGAWA and Y. TAKIZAWA, *Mol. Cryst. Liq. Cryst. Sci. Technol. Sect. A* **341** (2000) 357.
8. A. CORMA, *Chem. Rev.* **97** (1997) 2373.

9. C. T. LEE, M. H. UM and H. KUMAZAWA, *J. Amer. Ceram. Soc.* **83** (2000) 1098.
10. N. BAO, X. LU, X. JI, X. FENG and J. XIE, *Fluid Phase Equilibria*. **193** (2002) 229.
11. N. BAO, X. FENG, X. LU and Z. YANG, *J. Mater. Sci.* **37** (2002) 3035.
12. X. LU, X. JI, D. CHEN, C. LIU, N. BAO and X. FENG, *J. Chem. Ind. Eng. China* **53** (2002) 358.
13. X. JI, D. CHEN, T. WEI, X. LU, Y. WANG and J. SHI, *Chem. Eng. Sci.* **56** (2001) 7017.
14. M. H. UM, C. T. LEE and H. KUMAZAWA, *J. Amer. Ceram. Soc.* **84** (2001) 1181.
15. S. YIN, S. UCHIDA, Y. FUJISHIRO, M. AKI and T. SATO, *J. Mater. Chem.* **9** (1999) 1191.
16. J. LEE, K. LEE and H. KIM, *J. Mater. Sci.* **31** (1996) 5493.

*Received 26 September 2002
and accepted 28 January 2004*